



Mycobacterial Infection of Precision-Cut Lung Slices Reveals Type 1 Interferon Pathway Is Locally Induced by *Mycobacterium bovis* but Not *M. tuberculosis* in a Cattle Breed

Aude Remot^{1*}, Florence Carreras¹, Anthony Coupé¹, Émilie Doz-Deblauwe¹, Maria L. Boschioli², John A. Browne³, Quentin Marquant⁴, Delphine Descamps⁴, Fabienne Archer⁵, Abraham Aseffa⁶, Pierre Germon¹, Stephen V. Gordon⁷ and Nathalie Winter¹

OPEN ACCESS

Edited by:

Christophe J. Queval,
Francis Crick Institute,
United Kingdom

Reviewed by:

Graham Stewart,
University of Surrey, United Kingdom
Priscille Brodin,
Institut National de la Santé et de la
Recherche Médicale (INSERM),
France

*Correspondence:

Aude Remot
aude.remot@inrae.fr

Specialty section:

This article was submitted to
Veterinary Infectious Diseases,
a section of the journal
Frontiers in Veterinary Science

Received: 16 April 2021

Accepted: 02 June 2021

Published: 09 July 2021

Citation:

Remot A, Carreras F, Coupé A, Doz-Deblauwe É, Boschioli ML, Browne JA, Marquant Q, Descamps D, Archer F, Aseffa A, Germon P, Gordon SV and Winter N (2021) Mycobacterial Infection of Precision-Cut Lung Slices Reveals Type 1 Interferon Pathway Is Locally Induced by *Mycobacterium bovis* but Not *M. tuberculosis* in a Cattle Breed. *Front. Vet. Sci.* 8:696525. doi: 10.3389/fvets.2021.696525

¹ INRAE, Université de Tours, Nouzilly, France, ² Paris-Est University, National Reference Laboratory for Tuberculosis, Animal Health Laboratory, Anses, Maisons-Alfort, France, ³ UCD School of Agriculture and Food Science, University College Dublin, Dublin, Ireland, ⁴ INRAE, Université Paris-Saclay, UVSQ, Jouy-en-Josas, France, ⁵ INRAE, UMR754, Viral Infections and Comparative Pathology, IVPC, Univ Lyon, Université Claude Bernard Lyon 1, EPHE, Lyon, France, ⁶ Armauer Hansen Research Institute, Addis Ababa, Ethiopia, ⁷ UCD School of Veterinary Medicine and UCD Conway Institute, University College Dublin, Dublin, Ireland

Tuberculosis exacts a terrible toll on human and animal health. While *Mycobacterium tuberculosis* (Mtb) is restricted to humans, *Mycobacterium bovis* (Mb) is present in a large range of mammalian hosts. In cattle, bovine TB (bTB) is a noticeable disease responsible for important economic losses in developed countries and underestimated zoonosis in the developing world. Early interactions that take place between mycobacteria and the lung tissue early after aerosol infection govern the outcome of the disease. In cattle, these early steps remain poorly characterized. The precision-cut lung slice (PCLS) model preserves the structure and cell diversity of the lung. We developed this model in cattle in order to study the early lung response to mycobacterial infection. *In situ* imaging of PCLS infected with fluorescent Mb revealed bacilli in the alveolar compartment, in adjacent or inside alveolar macrophages, and in close contact with pneumocytes. We analyzed the global transcriptional lung inflammation signature following infection of PCLS with Mb and Mtb in two French beef breeds: Blonde d'Aquitaine and Charolaise. Whereas, lungs from the Blonde d'Aquitaine produced high levels of mediators of neutrophil and monocyte recruitment in response to infection, such signatures were not observed in the Charolaise in our study. In the Blonde d'Aquitaine lung, whereas the inflammatory response was highly induced by two Mb strains, AF2122 isolated from cattle in the UK and Mb3601 circulating in France, the response against two Mtb strains, H37Rv, the reference laboratory strain, and BTB1558, isolated from zebu in Ethiopia, was very low. Strikingly, the type I interferon pathway was only induced by Mb but not Mtb strains, indicating that this pathway may be involved in mycobacterial virulence and host tropism. Hence, the PCLS model in cattle is a valuable tool to deepen our understanding of early interactions between lung host cells and mycobacteria. It revealed striking differences

between cattle breeds and mycobacterial strains. This model could help in deciphering biomarkers of resistance vs. susceptibility to bTB in cattle as such information is still critically needed for bovine genetic selection programs and would greatly help the global effort to eradicate bTB.

Keywords: cattle, *Mycobacterium bovis*, *ex vivo*, precision cut lung slices, alveolar macrophages, type I interferon

INTRODUCTION

Bovine tuberculosis (bTB) caused by *Mycobacterium bovis* (Mb) remains one of the most challenging infections to control in cattle. Because of its zoonotic nature, this pathogen and its associated noticeable disease in cattle are under strict surveillance and regulation in the European Union. When bTB cases are detected through surveillance, culling of these reactor cattle is mandatory. In spite of intensive eradication campaigns, bTB is still prevalent in European cattle (1, 2) and has significant economic, social, and environmental implications. Since 2001, France is an officially bTB-free country, a status that was achieved through costly surveillance programs. However, each year, around 100 Mb foci of infection are identified (3), with certain geographical areas showing a constant rise in disease prevalence since 2004.

bTB eradication is an unmet priority that faces two major difficulties: the persistence of undetected infected animals in herds because of the lack of diagnostic sensitivity and the risk of transmission from infected sources (4). Moreover, the poor understanding of bTB pathophysiology in cattle and the lack of correlates of protection are substantial knowledge gaps that must be resolved so as to better tackle the disease (DISCONTTOOLS, <https://www.discontools.eu/>).

Both Mb and *Mycobacterium tuberculosis* (Mtb) belong to the same genetic complex. Mtb is responsible for tuberculosis (TB) in humans, which displays similar features with bTB. It is estimated that one-third of the global human population are latently infected with Mtb, which kills 1.4 million people each year (5). Despite the high degree of identity that Mtb and Mb share both at the genetic level as well as during the infection process, the two pathogens display distinct tropism and virulence depending on the host. While Mb is highly virulent and pathogenic for cattle and a range of other mammals, Mtb is restricted to sustain in humans. An experimental infection of cattle with the widely used Mtb laboratory strain H37Rv, which was genome-sequenced in 1998 (6), shows a strong attenuation compared to Mb (7, 8). However, the natural infection of cattle with Mtb has been reported, and the strain Mtb BTB1558 was once such a case, isolated from a zebu bull in Ethiopia (9, 10). In comparison to the original UK Mb strain AF2122/97, the first genome-sequenced Mb isolate (11, 12), the Mtb strain BTB1558 displayed a much lower virulence in European cattle (13).

The Mb strains that circulate in France today are phylogenetically distant from the UK Mb reference strain. While AF2122 belongs to the European 1 clonal complex (14), the European 3 clonal complex is widespread in France, (15). The Eu3 genetic cluster is composed of field strains that

share the SB0120 spoligotype with the attenuated Bacillus-Calmette-Guerin (BCG) vaccine strain (16, 17). In our study, we used Mb3601 as the representative strain of this widespread French cluster. Originally, Mb3601 was isolated from the tracheobronchial lymph node of an infected bovine in a bTB highly enzoonotic area in France (16). However, despite the widespread circulation in its original area, nothing is known today of the pathophysiology of Mb3601 infection.

Indeed greater knowledge is available on Mtb infection process and disease development both in humans and mouse models compared to Mb infection in cattle. With both mycobacteria, the alveolar macrophage (AMP) is the frontline cell that first presents the first niche for mycobacteria entering the lung, and the role of the AMP in early-stage infection is well established (8). Both Mtb and Mb have established their lifestyle in AMPs: they can escape its bactericidal mechanisms and multiply within this niche. During the infection process, bacilli disseminate to different anatomical sites and establish new infection foci both in the lungs and secondary lymphoid organs (18, 19). During Mtb infection, lung epithelial cells also play key roles in host defense [reviewed in (20–22)]. Type II pneumocytes are infected by Mtb (23) and produce pro-inflammatory cytokines which augment the AMP innate resistance mechanisms (24). The role of type II pneumocytes during Mb infection in cattle is not well known. Most of the available knowledge on the role of bovine macrophages (MPs) during Mb infection also comes from studies conducted with monocytes sampled from blood and derived as MPs during *in vitro* culture (25, 26).

In our study, we wanted to investigate the bovine innate response following Mb or Mtb infection in a preserved lung environment to allow the resident lung cells to interact with bacilli and crosstalk. Precision cut lung slices (PCLS) are an experimental model in which resident lung cell types are preserved and remain alive for at least 1 week (27). The tissue architecture and the interactions between the different cells are maintained. PCLS have already been validated for the study of various respiratory pathogens (27–29). In chicken PCLS, mononuclear cells are highly motile and actively phagocytic (30). This model is well designed to study complex interactions taking place early after the host–pathogen encounter. During Mb infection in cattle, important differences in the production of key proinflammatory cytokines such as IFN γ or TNF α by peripheral blood mononuclear cells are observed, depending on the clinical status of the animal. Interestingly, such differences are observed at early time points (31), indicating that the innate phase of the host response is key to the establishment of the pathological outcome of the infection.

Therefore, the PCLS model is ideally suited to investigate early host–pathogen interactions in the bovine lung during Mb infection and may help to find clues to the impact of the innate response on the outcome of infection. This model, which fully mimics the early environment of the bacillus entering the lung (compared to monocyte-derived MPs), may also aid in understanding the molecular basis of mycobacterial host preference (32). To this end, we decided to compare four mycobacterial strains: two Mtb species—namely, the Mtb H37Rv reference strain for human TB and the cattle derived Mtb BTB1558—and two Mb species—namely, Mb AF2122 as representative of the EU1 clonal complex and Mb3601 as the hallmark EU3 strain. Since the host genetic background also has a profound impact on the outcome of bTB disease (33), we decided to compare PCLS from two prevalent beef breeds in France—Charolaise and Blonde d’Aquitaine—and conducted a thorough characterization of the lung responses to Mb and Mtb during *ex vivo* infection. The PCLS allowed us to decipher important differences in the transcriptomic and cytokine profile during the innate response to infection, depending both on the breed, i.e., between Blonde d’Aquitaine and Charolaise cows, and on the mycobacterial species, i.e., between Mtb and Mb.

MATERIALS AND METHODS

Animal Tissue Sampling

Lungs from 15 Blonde d’Aquitaine and nine Charolaise cows were collected post-mortem at a commercial abattoir. The animals were between 3 and 11 years old and originated from eight different French departments where no recent bTB outbreak had been noticed (**Supplementary Figure 1**). No ethical committee approval was necessary as no animal underwent any experimental procedure. After slaughter by professionals following the regulatory guidelines from the abattoir, the lungs from each cow were systematically inspected by veterinary services at the abattoir. The origin of each animal was controlled, and its sanitary status was recorded on its individual passport: the animals were certified to be free of bTB, leucosis, brucellosis, and infectious bovine rhinotracheitis.

Bacterial Strains and Growth Conditions

Strains Mb AF2122/97 and Mb MB3601 had previously been isolated from infected cows in Great Britain and France, respectively (12, 15). The Mb3601-EGFP fluorescent strain was derived by electroporation with an integrative plasmid expressing EGFP and selected with Hygromycin B (50 µg/ml) (Sigma, USA) as described previously (34). Mtb BTB1558 had been previously isolated from a zebu bull in Ethiopia (13). Bacteria were grown in Middlebrook 7H9 broth (Difco, UK) supplemented with 10% BBLTM Middlebrook albumin–dextrose–catalase (BD, USA) and 0.05% Tween 80 (Sigma-Aldrich, St Louis, USA). At mid-log phase, the bacteria were harvested, aliquoted, and stored at –80°C. Batch titers were determined by plating serial dilutions on Middlebrook 7H11 agar supplemented with 10% oleic acid–albumin–dextrose–catalase (BD, USA), with 0.5% glycerol or 4.16 g/L sodium pyruvate (Sigma, USA) added for Mtb or Mb strains, respectively. The plates were incubated at 37°C for 3–4 weeks

(H37Rv, BTB558, and AF2122) and up to 6 weeks for Mb3601 before colony-forming unit (CFU) numeration. The inocula were prepared from one frozen aliquot (titer determined by CFU numeration) that was thawed in 7H9 medium without glycerol and incubated overnight at 37°C. After centrifugation for 10 min at 3,000 × g, the concentration was adjusted to 10⁶ CFU/ml in RPMI medium.

Obtention and Infection of Precision-Cut Lung Slices

PCLS were obtained from fresh lungs using a tissue slicer, MD 6000 (Alabama Research and Development). For each animal, the right accessory lobe was filled *via* the bronchus with RPMI containing 1.5% low-melting-point (LMP) agarose (Invitrogen) warmed at 39°C. After 20 min at 4°C, the solidified lung tissue was cut in 1.5-cm slices with a scalpel. A 0.8-mm diameter-punch was used to obtain biopsies that were placed in the microtome device of the Krumdieck apparatus, filled with cold phosphate-buffered saline (PBS), and 100-µm-thick PCLS were cut. One PCLS was introduced in each well of a 24-well plate (Nunc); 1 ml of RPMI 1640 (Gibco) supplemented with 10% heat-inactivated fetal calf serum (FCS, Gibco), 2 mM L-glutamine (Gibco), and PANTA™ antibiotic mixture (polymyxin B, amphotericin B, nalidixic acid, trimethoprim, and azlocillin; Becton Dickinson) was added to the well, and the plate was incubated at 37°C with 5% CO₂. The medium was changed every 30 min during the first 2 h to remove all traces of LMP agarose. At 24 h later, after the last medium change, ciliary activity was observed under a microscope to ensure tissue viability.

The PCLS were infected for 2 days with 10⁵ CFU of Mb or Mtb strains. As indicated, the PCLS were either fixed in formalin for imaging or lysed with a Precellys in lysing matrix D tubes in 800 µl Tri-reagent for RNA extraction. The bacillary load of each strain present in the PCLS was compared after the transfer of the PCLS to a new plate at 1 day after infection (dpi), two washes in 1 ml of PBS, and homogenization in 1 ml of PBS in lysing matrix D tubes (MP Biomedicals) with a Precellys (Ozyme). To determine CFUs, serial dilutions were plated as described above.

Alveolar Macrophages

To harvest alveolar macrophages (AMPs) from Blonde d’Aquitaine cows, broncho-alveolar lavages (BAL) were performed on the left basilar lobe of the lung at a local abattoir after culling the animal. The lobe was filled with 2 × 500 ml of cold PBS containing 2 mM EDTA (Sigma-Aldrich). After the massage, the BAL was collected and transported at 4°C to the laboratory. BAL was filtered with a 100-µm cell strainer (Falcon) and centrifuged for 10 min at 300 × g. The cells were washed in RPMI medium supplemented with 10% heat-inactivated fetal calf serum (Gibco), 2 mM L-glutamine (Gibco), and PANTA™ Antibiotic Mixture. Then, 10⁷ BAL cells per milliliter were suspended in 90% FCS and 10% dimethyl sulfoxide (Sigma-Aldrich) and cryopreserved in liquid nitrogen. At 1 day before infection, the BAL cells were thawed at 37°C, washed in complete RPMI medium, and transferred to a 75-cm² culture flask with a ventilated cap. After 2 h at 37°C and 5% CO₂, non-adherent cells were removed, and adherent AMPs were incubated 2 × 10 min

at 4°C with 10 ml of cold PBS to detach and enumerate them in a Malassez chamber. Then, 5×10^5 AMPs/well were distributed in a 24-well plate and incubated overnight at 37°C and 5% CO₂. The medium was changed once, and AMPs were infected with Mb3601 or Mtb H37Rv at a multiplicity of infection (MOI) of 1. At 6 and 24 h post-infection, the supernatants were filtered through a 0.2-μm filter, and the cells were lysed in 800 μl of Tri-reagent for RNA extraction. The MOI was checked by CFU determination at 24 h after infection.

Cell Supernatant Collection and Lactate Dehydrogenase Assay

In order to evaluate cytotoxicity, supernatants from infected PCLS or AMPs were passed through a 0.2-μm filter at indicated time points, and cells were lysed in 1 ml of lysis buffer (5 mM EDTA, 150 mM NaCl, 50 mM Tris-HCl, Triton 1%, pH 7.4), containing anti-proteases (Roche), in a lysing matrix D tube, with a Precellys apparatus. The homogenates were clarified by centrifugation for 10 min at $10,000 \times g$, filtered through 0.2 μm, and collected on microplates. The cytotoxicity of infection in PCLS was assessed using the Non-radioactive Cytotoxicity Assay kit (Promega) according to the manufacturer's instructions. The cytotoxicity was calculated as cytotoxicity (%) = $[\text{OD}_{490} \text{ of lactate dehydrogenase (LDH) in the supernatant}] / (\text{OD}_{490} \text{ of LDH in the supernatant} + \text{OD}_{490} \text{ of LDH in the PCLS homogenates}) \times 100$.

Immunohistochemistry on PCLS

The infected PCLS were fixed 24 h at 4°C with 4% formalin and then transferred to a 48-well culture plate in PBS. All steps that will be described below were done under gentle agitation at room temperature (RT). The PCLS were incubated for 2 h with 100 μl of PBS, 0.25% Triton X-100, and 10% horse serum for permeabilization and saturation (saturation buffer). They were incubated overnight at 4°C with primary Ab (anti-bovine MHCII clone MCA5655 from BioRad and anti-bovine pancytokeratine clone BM4068 from Acris) diluted in saturation buffer. The PCLS were washed four times with 300 μl of PBS (two times for 5 min and then two times for 10 min) and then incubated for 3 h with fluorescent-conjugated secondary antibodies diluted in saturation buffer (goat anti-mouse IgG1-APC and goat anti-mouse IgG2a A555 from Invitrogen). The PCLS were washed four times with 300 μl of PBS (two times for 5 min and then two times for 10 min), transferred on cover slides which were mounted with Fluoromount-GTM mounting medium containing DAPI (Invitrogen), and sealed with a transparent nail polish. Z-stack imaging was performed at $\times 63$ enlargement with a confocal microscope (LEICA) and analyzed with LAS software. The presence/absence of Mb and number of macrophages per alveoli were numerated by eye at the confocal microscope, with one person counting and the other confirming and reporting the data.

Quantification of Cytokines and Chemokines Released by PCLS and AMPs

The cytokine and chemokine levels produced by PCLS after 2 dpi were assessed in a Multiplex assay in supernatants (dilution 1:2) with MILLIPLEX[®] Bovine cytokine/chemokine panel 1 (BCYT1-33K-PX15, Merck) according to the manufacturer's

instructions. IFN γ , IL-1 α , IL-1 β , IL-4, IL-6, IL-8 (CXCL8), IL-10, IL-17A, IL-36RA (IL-1F5), IP-10 (CXCL10), MCP-1 (CCL2), MIP-1 α (CCL3), MIP-1 β (CCL4), TNF α , and VEGF-A were measured. Data were acquired using a MagPix instrument (Luminex) and analyzed with Bio-Plex Manager software (Bio-Rad). IL-8 was out of range in the Multiplex, so we performed a sandwich ELISA with the following references: goat anti-bovine interleukin-8 Ab AHP2817, recombinant bovine interleukin-8 PBP039, and goat anti-bovine interleukin-8 Ab conjugated to biotin AHP2817B (all from Bio-Rad), following the protocol according to the manufacturer's instructions.

RNA Extraction and Gene Expression Analysis

The total RNA from two pooled PCLS was extracted using a MagMAXTM-96 Total RNA isolation kit (ThermoFisher). For AMPs, we used the Nucleospin RNA isolation kit (Macherey Nagel). After DNase treatment (ThermoFisher or Macherey Nagel), the mRNAs were reverse-transcribed with iScriptTM Reverse Transcriptase mix (Biorad) according to the manufacturer's instructions. The primers (Eurogentec; **Supplementary Table 1**) were validated, using a serially diluted pool of cDNA mix obtained from bovine lung, lymph nodes, blood, and bone marrow, with a LightCycler[®] 480 Real-Time PCR System (Roche). Gene expression was then assessed with the BioMark HD (Fluidigm) in 96×96 -well integrated fluidic circuit plate according to the manufacturer's instructions. The annealing temperature was 60°C. The data were analyzed with Fluidigm RealTime PCR software to determine the cycle threshold (Ct) values. The messenger RNA (mRNA) expression was normalized to the mean expression of three housekeeping genes (*PPIA*, *GAPDH*, and *ACTB*) to obtain the ΔCt value. For each animal, values from infected PCLS were normalized to the uninfected PCLS gene expression ($\Delta\Delta\text{Ct}$ value and relative quantity = $2^{-\Delta\Delta\text{Ct}}$). Principal component analysis (PCA) was performed using $\Delta\Delta\text{Ct}$ values in R studio (version 1.1.456, ©2009–2018 RStudio, PBC) using the FactoMineR packages (version R 3.5.3).

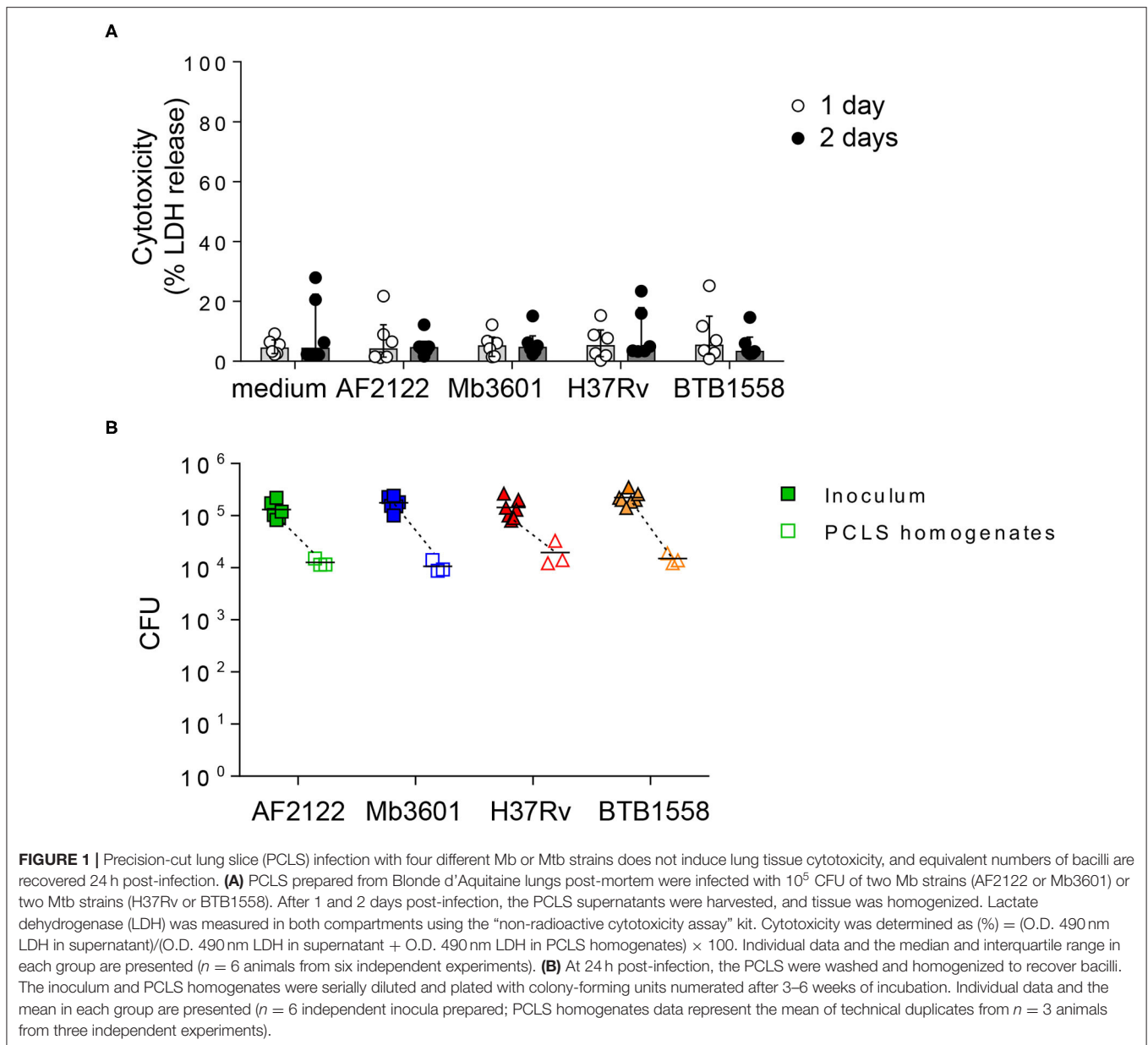
Statistical Analysis

The individual data and the median and interquartile range are presented in the figures, except for **Figure 2** where the mean and standard error of the mean (SEM) are presented. Statistical analyses were performed with Prism 6.0 software (GraphPad). Analyses were performed on data from two to six independent experiments, with two-way ANOVA or Wilcoxon non-parametric tests for paired samples used. The represented *p*-values were **p* < 0.05, ***p* < 0.01, and ****p* < 0.001.

RESULTS

Ex vivo Infection With Mycobacteria of Live Bovine Lung Tissue in PCLS Allows Bacilli Uptake by AMPs and Their Recruitment to the Alveoli

The early events of bTB pathophysiology in the bovine lung remain poorly defined due to the complexity of biocontained experimental infection in large animals. Since PCLS have been

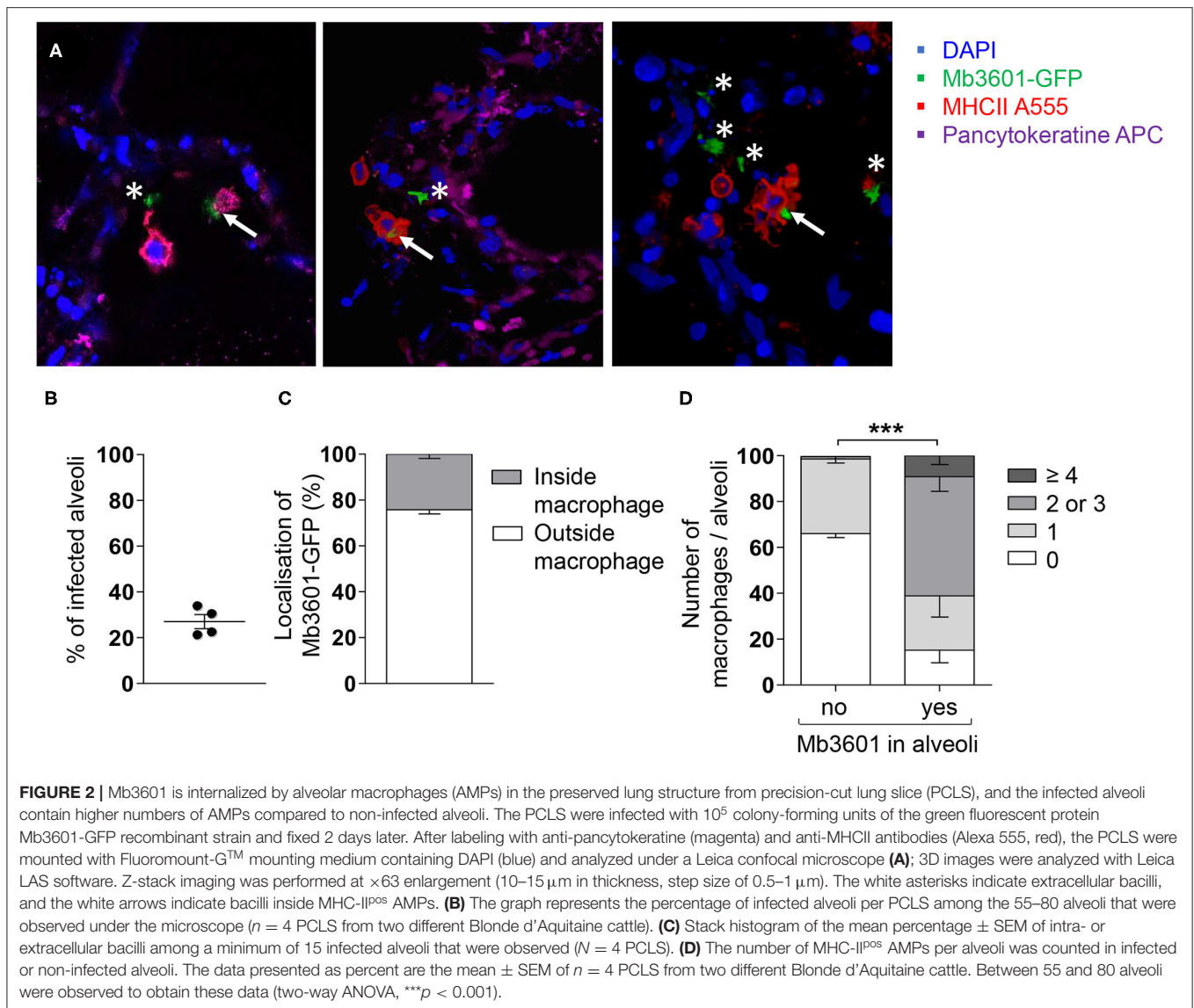


used to study viral respiratory infections in the bovine (27), we decided to use this model to assess early events taking place following entry of Mb into the lung. We infected bovine PCLS obtained *ex vivo* with the four mycobacterial strains: Mb AF2122, Mb3601, Mtb H37Rv, or BTB1558.

We first monitored tissue cytotoxicity at 1 and 2 dpi using a LDH release assay. The mean percentage of cytotoxicity remained below 10%, and no difference was observed between infected and non-infected PCLS (**Figure 1A**). The ciliary activity from the PCLS bronchial cells monitored every day under a light microscope remained vigorous and stable after infection (data not shown). We calibrated our model and inocula to use 10^5 CFUs for each of the four different strains. We analyzed CFUs still present in PCLS at 24 h later and observed an equivalent

1 log decrease for all strains (**Figure 1B**). This indicated an equivalent infection by all strains, allowing them to be directly compared. Therefore, with a similar bacterial load and excellent tissue viability in all experimental conditions, we validated PCLS as a model to study the early events taking place in the bovine lung after infection with mycobacteria.

In order to visualize the interactions taking place between bacilli and lung cells, we infected the PCLS with a fluorescent version of the Mb3601 strain, and at 1 and 2 dpi, we analyzed the cells by *in situ* immunohistochemistry. The lung structure was visualized by DAPI and pancytokeratine staining, and we used confocal microscopy to image 10–15- μm sections and localize Mb3601-EGFP (**Figure 2A**). We observed Mb in $27 \pm 3\%$ of PCLS alveoli (**Figures 2A,B**) and almost always in

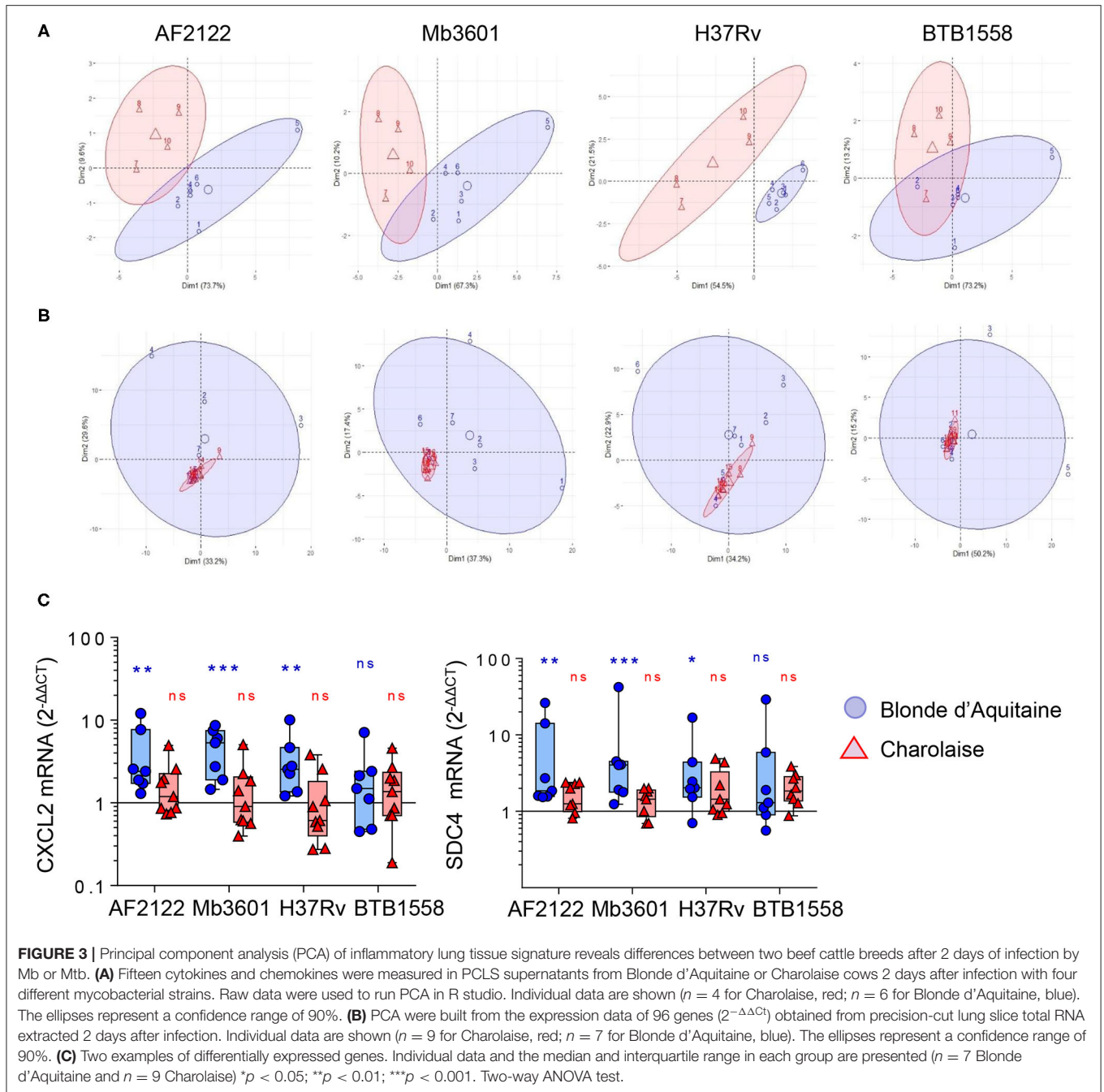


close contact with large MHC-II-positive AMPs. The bacilli were localized outside AMPs in $76 \pm 2\%$ observations and resided intracellularly in AMPs in $24 \pm 2\%$ (Figures 2A,C and Supplementary Video 1). Interestingly, the number of AMPs per alveoli differed upon bacilli presence or absence (Figure 2D). In uninfected PCLS, lung alveoli generally contained one AMP (data not shown). However, in Mb-infected PCLS, we either observed no AMPs in $66 \pm 2\%$ of alveoli or one AMP in $33 \pm 2\%$ of alveoli in the absence of any Mb. On the contrary, the number of AMPs significantly increased in alveoli where at least one Mb was observed (Figure 2D, $p < 0.001$). The number of AMPs varied among infected alveoli, with $24 \pm 9\%$ containing one AMP, $52 \pm 6\%$ containing two or three AMPs, and $9 \pm 4\%$ containing more than four AMPs. Such observations indicated that, during the 2 days of infection, AMPs were recruited from one alveolus to another in response to signals linked to Mb infection. In conclusion, even though Mb infection

was performed *ex vivo*, bacilli were observed in the alveoli, close or inside their target host cell, i.e., the AMP. Moreover, the PCLS model was physiological enough to allow AMPs to crawl in response to signals linked to bacilli entry.

The Lung Response to Mycobacterial Infection Vastly Differs Between Blonde d'Aquitaine and Charolaise Cows

Two bovine beef breeds are widely used in France: Blonde d'Aquitaine and Charolaise. We decided to compare how these two breeds respond to mycobacterial infection, using our PCLS system. We measured 15 cytokines and chemokines secreted by the lung tissue at 2 dpi with the four mycobacterial strains and performed a PCA. As depicted in Figure 3A, the PCA revealed important differences in the immune response of the lung tissue between the two breeds. The group samples clearly



plotted apart, and their ellipses showed either a small overlay (AF2122 and Mb3601) or no overlay at all (H37Rv). The results for the BTB1558 group showed less clustering of samples due to higher individual variations. We then extracted total RNA from PCLS after 1 or 2 dpi and analyzed the expression of 96 genes related to innate immunity and inflammation (see the full list in **Supplementary Table 1**). The RT-qPCR data were normalized and expressed as fold change compared to uninfected PCLS control for each cow. Gene expression was higher at 2 days after infection compared to that at 1 dpi (data not shown). We

therefore decided to focus our analysis on this 2-dpi time point. Remarkably, the transcriptomic signature induced by infection was very low for the Charolaise breed, whichever mycobacterial strain was used, which explains the clustering of Charolaise samples (**Figure 3B**). Increasing the inoculum in the Charolaise PCLS up to 5×10^6 CFU did not induce gene expression (**Supplementary Figure 2**). The response of the lung tissue to mycobacterial infection in Blonde d'Aquitaine was very different compared to that in Charolaise as revealed by a PCA (**Figure 3B**). Whereas, in PCLS from Charolaise the gene expression from

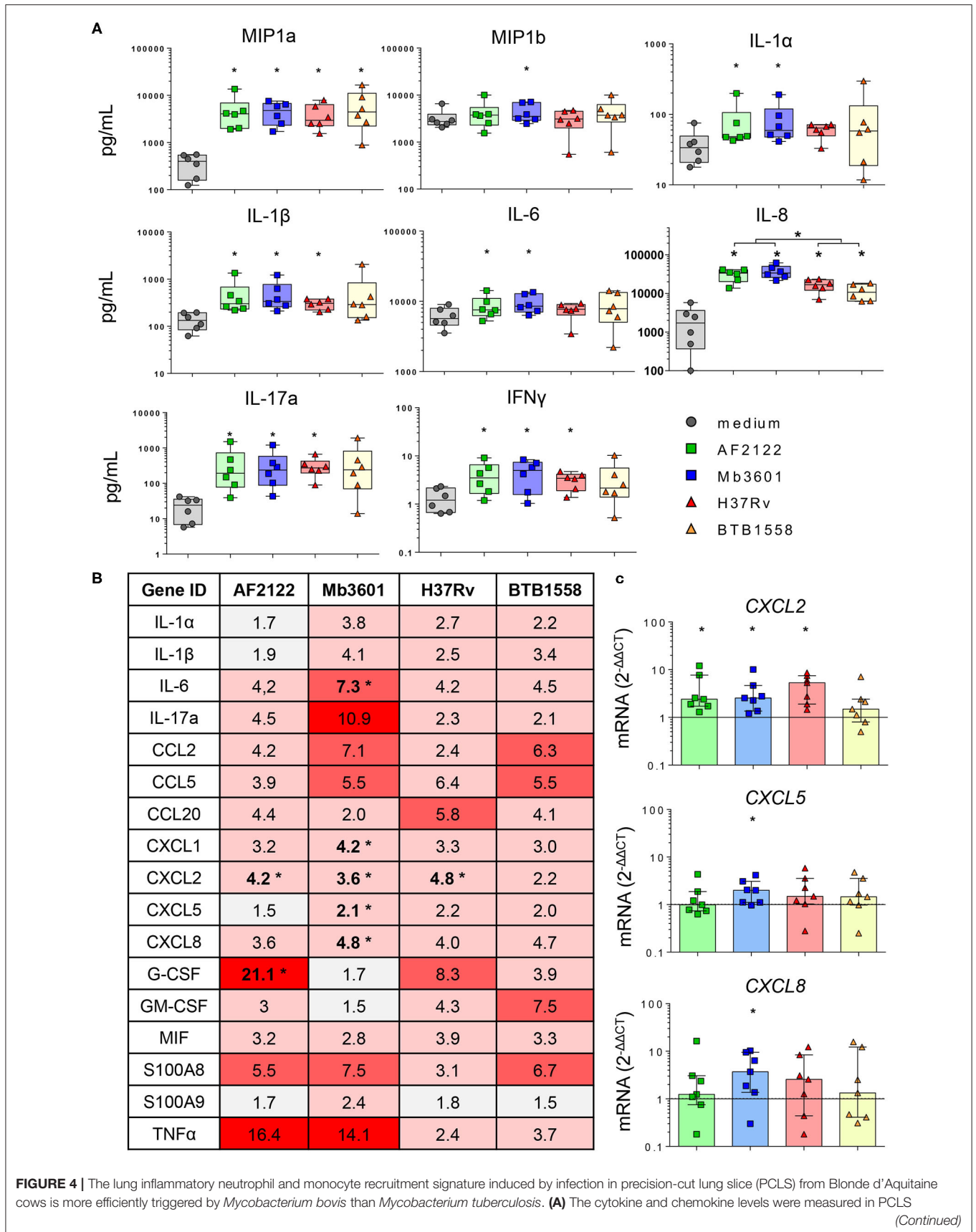


FIGURE 4 | supernatant by Multiplex ELISA 2 days after infection with two Mb or two Mtb strains. Individual data and the median and interquartile range in each group are presented ($n = 6$ cows). **(B)** Table of the mean of fold change ($2^{-\Delta\Delta CT}$) for each group ($n = 7$ cows) of 17 major genes involved in neutrophil and monocyte recruitment and inflammation. The graduated red box coloring represents levels of gene expression, and the asterisks mark significant differences compared to non-infected controls. **(C)** *CXCL2*, *CXCL5*, and *CXCL8* gene expression at 2 days post-infection. Individual data and the median and interquartile range in each group are presented ($n = 7$ cows). **(B,C)** * $p < 0.05$ (Wilcoxon nonparametric test).

infected and non-infected controls clustered, in PCLS from Blonde d'Aquitaine, the gene expression levels were significantly more dispersed after infection compared to those of controls (**Figure 3B**). We compared the individual gene expression between the two breeds for a number of genes. For instance, both the *CXCL2* chemokine and the mycobacteria receptor syndecan 4 *SDC4* were significantly upregulated after PCLS infection with AF2122, Mb3601, or H37Rv in Blonde d'Aquitaine, but not in Charolaise (**Figure 3C**). Our data altogether revealed important differences in the early lung response to mycobacterial infection, depending on the breed of the animals, that could be measured both at the gene expression and protein production level in the PCLS system.

The Overall Inflammation Signature in the Lung Tissue Is Triggered More Efficiently by *M. bovis* Than *M. tuberculosis*

We then focused our analysis on Blonde d'Aquitaine to determine how the lung tissue responded to different mycobacterial strains. We analyzed 15 cytokines and chemokines produced in the PCLS supernatants 2 days following an infection. No IL-4 was detected, and the production of TNF α , IL-36RA, IL-10, VEGFA or MCP-1 was not different between infected PCLS and controls (**Supplementary Figure 3A**). We observed that *ex vivo* infection of PCLS with mycobacteria triggered an inflammatory response that contrasted between the strains (**Figure 4A**). At the protein level, the Mtb strain BTB1558 induced the most heterogeneous response, and due to high individual variation, differences in chemokine/cytokine production between infected PCLS and controls only reached a statistical significance for MIP-1a (CCL3) and IL-8 (**Figure 4A**). These two inflammatory mediators were also strongly induced by all strains. IL-17A, IL-1 β , and IFN γ were efficiently induced by mycobacterial infection, and no significant difference was observed between Mtb and Mb. By contrast, IL-6 and IL-1 α were significantly induced after Mb, but not Mtb, infection, and IL-8 production was also significantly higher after Mb than Mtb infection (**Figure 4A**). The only strain able to induce a significant production of MIP-1b was Mb3601. We then analyzed the inflammatory transcriptomic signature using a panel of 17 genes involved in monocyte/macrophage and neutrophil recruitment (**Figure 4B**). A number of these genes was significantly upregulated upon PCLS infection even though significant differences were not always reached due to inter-individual variation. Remarkably, Mb3601 induced the strongest inflammatory response, with five out of 17 genes significantly upregulated compared to non-infected controls. Focusing on chemokines involved in neutrophil recruitment, we observed that *CXCL2* expression was induced by all strains—except

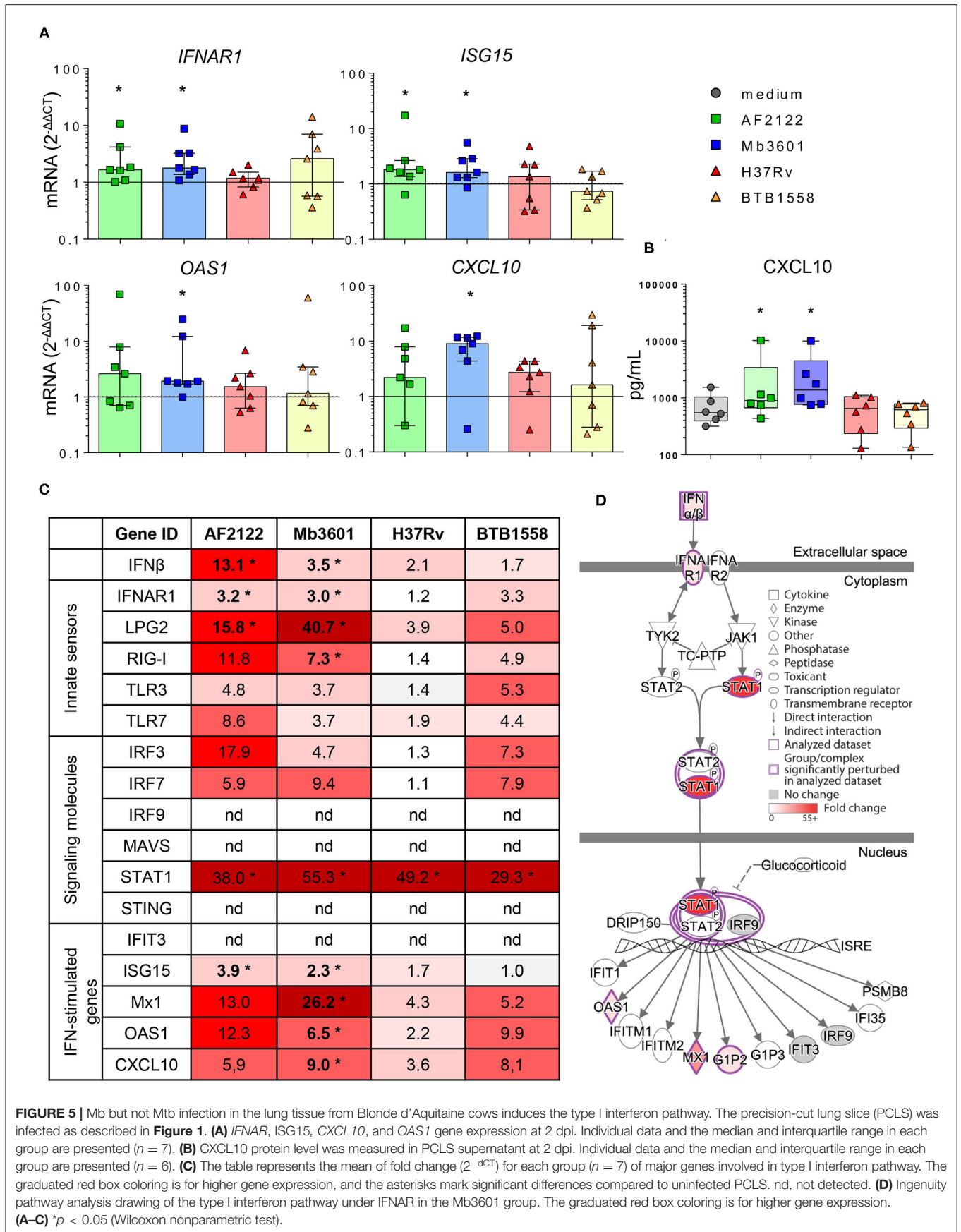
BTB1558—whereas *CXCL1*, *CXCL5*, and *CXCL8* were only upregulated by Mb3601 (**Figures 4B,C**). *IL-6* expression was also high after Mb3601 infection. Therefore, the *ex vivo* infection of PCLS efficiently triggered signals involved in monocyte and neutrophil recruitment. Infection by Mb strains, more specifically the Mb3601 strain circulating in France, triggered inflammation in the bovine lung more efficiently than Mtb.

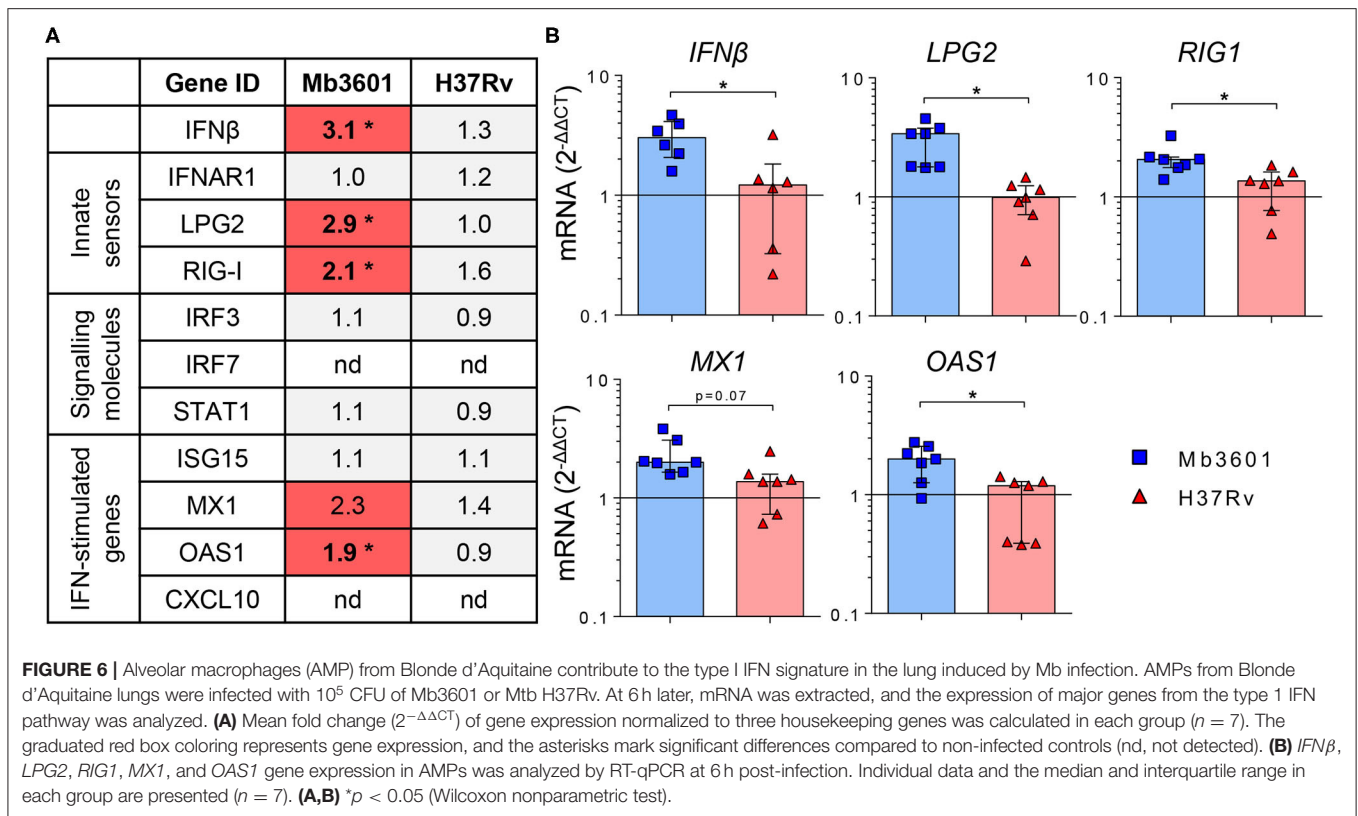
The Type I Interferon Pathway Is Induced in the Bovine Lung by Infection With *M. bovis*, but Not *M. tuberculosis*

Because in humans and mouse models susceptibility to mycobacterial infection and disease progression is driven by type I IFN (35–37), we decided to compare the induction of this pathway by Mtb and Mb strains in bovine lung tissue. We measured the expression of different genes involved in the type I IFN pathway in Blonde d'Aquitaine PCLS infected by the four mycobacterial strains (**Figure 5**). The gene expression of both *IFN β* and the *IFNAR1* receptor was significantly increased after Mb but not Mtb infection (**Figures 5A,C**). Similarly, the major IFN-stimulated genes (ISG) *MX1*, *OAS1*, *ISG15*, and *CXCL10* were induced only after Mb infection (**Figures 5A,C**), and this difference was also detected at the protein level for *CXCL10* (**Figures 5A,B**). Therefore, we observed the induction of a number of genes of the type I IFN pathway, recapitulated in **Figure 5D**, after infection with Mb, but not Mtb, strains. Strikingly, strain Mb3601 was the highest inducer of this pathway in the lung from Blonde d'Aquitaine cows.

Because AMPs are the most prominent host cells interacting with Mb (8), which we also observed in PCLS (**Figure 2**), we next decided to decipher if AMPs contributed to the induction of the type I IFN pathway after Mb3601 or H37Rv infection. At 1 day after the infection of AMPs with these two strains, similar bacterial levels were recovered (data not shown). At 6 h post-infection, no cell cytotoxicity was observed, and we analyzed the expression of genes from the type I IFN pathway at this early time point. While we did not observe differences in *IFNAR1*, *IRF3*, *STAT1*, nor *ISG15* expression induced by the two strains (**Figure 6A**), *IFN β* , *LPG2*, *RIG1*, and *OAS1* were significantly induced after infection with Mb3601, but not H37Rv (**Figure 6B**). Regarding *MX1*, the same trend was observed, although statistical significance was not reached (**Figure 6B**, $p = 0.07$).

Interestingly, while *CXCL10* was detected both at the mRNA and protein levels in PCLS infected with Mb (**Figure 5**), we did not detect the expression of this gene by AMPs in our analysis. These results altogether demonstrate that AMPs globally contribute to the type I IFN pathway in the lung after Mb infection, although other cells present in PCLS may also





specifically induce some genes, such as *CXCL10* or *IRF7*, for example (Figures 5C, 6A).

DISCUSSION

The lung is the main organ targeted by Mb infection in cattle (38), and early interactions between the different lung cell types and the bacillus that govern the pathophysiology of the disease need to be better understood. In this study, we used PCLS for the first time to monitor the early bovine lung response to Mb infection and validated this model as a means to measure the local innate response at the protein and mRNA level. A main advantage of PCLS is conservation of the complex lung tissue both in structure and diversity of cell types. After infection with mycobacteria, the ciliary activity of bronchial cells was maintained. The AMP main function is to patrol the lung, crawling in and between alveoli; they sensed, chemotaxed, and phagocytosed debris or inhaled bacteria (39). We observed increased numbers of AMPs in alveoli where Mb was present, indicating AMP mobility inside the tissue. In chicken, PCLS allowed the observation of the movement of macrophages and phagocytosis (30). The AMP is well established as the main host cell for Mtb infection in humans (40) and Mb infection in cattle (41). Accordingly, in PCLS, we observed Mb inside AMPs in 20% of infected alveoli. We sometimes observed several bacilli inside one AMP. Although Mb is able to replicate inside this hostile cell, it is difficult to know if this observation was due to bacillary multiplication or the phagocytosis of several

bacilli. This issue would need live imaging of PCLS to follow the fate of fluorescent Mb, an approach which remains challenging under BSL3 conditions.

In uninfected PCLS, we observed generally one AMP for two to three alveoli [Supplementary Figure 4; in good correlation with the observations of Neupane et al. (39)]. After Mb infection, we observed several AMPs inside the same alveolus in 50% of cases. Moreover, when the alveoli contained more than four AMPs, they were in close contact. Multinucleated giant cells are formed by the fusion of several MPs and are a hallmark of TB pathophysiology. It has recently been demonstrated that, after infection of human or bovine blood-derived MPs by Mb or Mtb, only Mb was able to induce the formation of multinucleated cells (26). Although at 2 dpi we did not observe the formation of such cells in PCLS, it would be interesting to analyze if such events could be detected after longer infection periods. Goris et al. have maintained bovine PCLS during 1 week to study viral infections (27).

One other advantage of our model is the preserved diversity of lung cell composition. PCLS contain type I and II pneumocytes, endothelial cells, and bronchial cells (Supplementary Figure 4) and also produce key molecules like surfactant, which has an established role in Mtb uptake (42). Mtb is also capable of invading type II alveolar epithelial cells (23) that play important roles in host defense (20–22). In our study, we did not observe intraepithelial Mb, but specific labeling of bovine epithelial cells would be required to investigate interactions between bovine lung pneumocytes and Mb in more detail. However, as we have

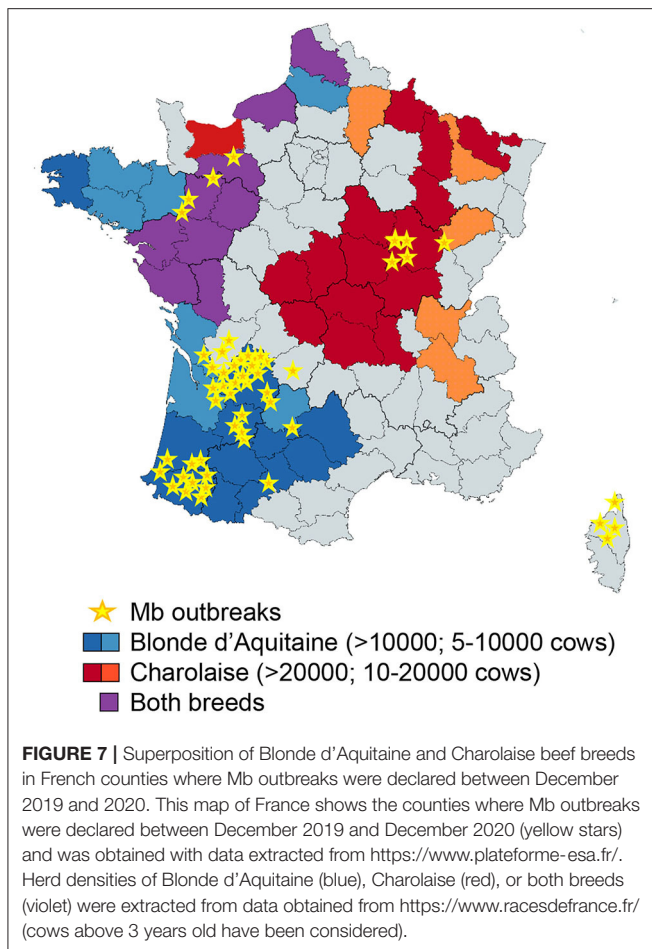
observed that infected AMPs were in close contact with epithelial cells in PCLS, this model will allow a more refined analysis of the crosstalk between AMPs and pneumocytes during Mb infection (24).

One limitation of the PCLS model is the lack of recruitment of immune cells from circulating blood. During mycobacterial infection, in response to local signals, a variety of immune cells are recruited to the infection site to form the mature granuloma that constrains bacillary multiplication. How this response is orchestrated at the level of the lung tissue in cattle remains poorly established. Neutrophils, together with other innate cells, such as macrophages, $\gamma\delta$ -T lymphocytes, and natural killer cells, were recently identified as key immune cells in the early containment of infection (43) and development of early lesions (44). Moreover, humans regularly exposed to Mtb or cattle exposed to Mb do not always develop signs of infection, i.e., remain negative in IFN γ -release assay or skin testing. In humans, such resistance to infection through the successful elimination of bacilli could be mediated by neutrophils (45). Similarly, in cattle experimentally infected with Mb, some contact animals resist infection, while others develop lesions due to productive infection (46). It is possible that neutrophils could also play an important role in the early elimination of Mb in cattle (43). Immune signals involved in the early recruitment of neutrophils to the lung after the entry of Mb need to be better understood in cattle. It is known that epithelial cells secrete, among other cytokines and chemokines, MIP1 and CXCL8 that attract MPs and neutrophils to the site of infection. Interestingly, we measured important differences in the production of such mediators by PCLS in response to different strains of mycobacteria that could be linked to variable virulence. Although one cattle type II pneumocyte cell line has been described (47), such transformed cells are less physiologically relevant than primary cells. Recently, immortalized type II cells were co-cultured with endothelial cells as a model of the bovine alveolus to study mycobacterial interactions with BCG. In this study, the authors detected the production of IL-8, TNF α , IL-22, and IL-17a. One limitation of this model was epithelial cell death, which occurred shortly after infection (48). As a physiological model, PCLS could help in understanding the early orchestration of the local inflammatory response in the lung in response to mycobacterial infection.

Resistance to bTB is linked to the host genetics. Zebu breeds (*Bos indicus*) are more resistant to bTB disease than *Bos taurus*-derived breeds (49). Our results with PCLS, as a physiological model of the early lung response to infection, demonstrated striking differences between Blonde d'Aquitaine and Charolaise, emphasizing the importance of host genetics in response to Mb. It is not known whether the stronger inflammatory response of the Blonde d'Aquitaine tissue is associated with a greater sensitivity or resistance to Mb infection. While robust immunological responses are associated with an increased pathology at the level of the animal (31), at the cellular level, blood-derived MPs from animals with greater resistance to bTB (and that kill BCG more efficiently than cells from susceptible animals) produce higher levels of the pro-inflammatory mediators iNOS, IL-1 β , TNF α , MIP1, and MIP3 (25). Although genetic selection of cattle would greatly complement bTB management and

surveillance programs to control and ultimately eradicate the disease, especially in countries with the highest burden (50, 51), biomarkers to evaluate the resistance or susceptibility of cattle to Mb infection are critically missing. Some genomic regions and candidate genes have been identified in Holstein-Friesian cows, the most common dairy breed (52), and not surprisingly, these candidates are often involved in inflammation. A genomic region on chromosome 23, containing genes involved in the TNF α /NF κ -B signaling pathway, was strongly associated with host susceptibility to bTB infection (53). However, large within-breed analyses of Charolaise, Limousine, and Holstein-Friesian cattle identified 38 SNPs and 64 QTL regions associated with bTB susceptibility to infection (54). The genotyping of 1966 Holstein-Friesian dairy cows that were positive by skin test and either did or did not harbor visible bTB lesions, together with their skin test negative matched controls, led to the conclusion that these variable phenotypes following Mb exposure were governed by distinct and overlapping genetic variants (55). Thus, variation in the pathology of Mb seems to be controlled by a large number of loci and a combination of small effects. Similar conclusions were drawn from the genetic studies of human tuberculosis (56). In areas where Mb is highly prevalent, recurrent exposure to Mb may also imprint the bovine genome, and epigenetics could also contribute to the immune response in certain breeds. In France, the Nouvelle Aquitaine region accounted for 80% of Mb outbreaks last year. Interestingly, Blonde d'Aquitaine breed is very abundant in this area (Figure 7). Together with Limousine, another very abundant beef breed in this region, they contribute to most bTB outbreaks in Nouvelle Aquitaine (bovine tuberculosis national reference laboratory communication). In the future, comparisons between Blonde d'Aquitaine and Limousine would be interesting. In our study, Blonde d'Aquitaine or Charolaise cows were sampled from eight different French departments, none with recurrent Mb outbreaks, rendering previous exposure to Mb unlikely. Moreover, the breeding management was similar for the two breeds, as far as we could ascertain, suggesting that exposure to environment and possible wildlife sources would be comparable. We nevertheless observed striking differences in the early lung response to Mb infection between these two breeds, pointing to the possible control of Mb infection at the genetic or epigenetic level. Whether some cattle breeds are more susceptible to bTB than others remains an open question that deserves future studies with more consequent animal sampling. We furthermore believe that the PCLS model could greatly contribute to unraveling the role of tissue-level protective responses that would, in turn, reveal important biomarkers.

In addition to the cattle breed, our study pointed toward differences in the host response to distinct mycobacterial strains. The Mb strains were better inducers of a lung immune response than Mtb in cattle, which is in agreement with a previous work showing that Mtb H37Rv was attenuated *in vivo* in cattle compared to Mb AF2122 (13). *In vitro* studies with bovine AMPs infected with AF2122 or H37Rv revealed differences in the innate cytokine profiles: the CCL4, IL-1 β , IL-6, and TNF α levels were more elevated in response to AF2122 than H37Rv (8), which is in agreement with our data. Interestingly, Mb3601,



a representative strain of a highly successful genetic cluster that circulates both in cattle and wildlife in France (16), induced an inflammatory signature in the lung more efficiently than Mb AF2122. Whether this correlates with differences in Mb virulence in cattle or other mammals remains to be investigated; but, if this were the case, the PCLS model would be a practical tool to study and compare the virulence of Mb field strains compared to the *in vivo* experimental infection of cattle. Contrary to Mtb which is mostly restricted to humans, Mb is adapted to sustain across a large host range through repeated cycles of infection and transmission (57, 58). This remarkable trait is due to pathogen molecular genetic changes (59) that allow adapted bacilli to manipulate the host immune response to establish infection and disease and ultimately transmit infection to new, susceptible hosts (60, 61). We observed a weaker inflammation in the bovine lung after infection with Mtb compared to Mb, and it will be interesting to compare the ability of Mtb and Mb to induce inflammation in human PCLS obtained post-surgery. This latter comparative analysis could give clues on the links between lung innate inflammatory responses and host adaptation during TB.

Our most striking observation was the Mb-restricted induction of the type I IFN pathway in the bovine lung. This is in agreement with previous studies in bovine AMPs where cytosolic

DNA-sensing pathways, in particular, RIG-I, were activated after 48 h of infection by Mb AF2122, but not Mtb H37Rv (32). In agreement with our data, these authors also demonstrated an induction of the RIG-I signaling pathway by Mb in AMPs (62). Therefore, AMPs contribute to type I IFN signaling in the lung. However, we also noticed differences between PCLS and AMPs in the induction of the IFN signature by Mb: for example, CXCL10 was detected in PCLS, but not in AMPs, in our study, which may be due to the time point used (63). However, it is also possible that other cells involved in crosstalk with AMPs contributed to CXCL10 production in response to Mb infection. Since CXCL10 has been proposed as a diagnostic biomarker of Mb infection in cattle (64), it will be interesting to better understand how this key mediator is regulated. Type I interferon favors Mb survival, and its induction may be a good manipulation strategy for the maintenance of infection. This manipulation mechanism, deciphered *in vitro* in murine bone marrow monocyte-derived MPs, involves the triggering of autophagy by cytosolic Mb DNA, in turn inducing IFN β production. Autophagy antagonizes inflammasome activation to the benefit of Mb survival (65, 66). In C57BL/6 mice treated with IFNAR1 blocking Ab and infected with Mb, the recruitment of neutrophils was reduced, but the pro-inflammatory profile of MPs was increased, leading to a reduced bacillary burden (67). No impact on T-cells was observed in this *in vivo* model, revealing a role of type I IFN signaling during the innate phase of the host response to infection. Therefore, Mb exploits type I IFN signaling in many ways, and this pathway seems an important avenue to better understand Mb virulence. The PCLS model will greatly help to better dissect out this pathway in the lung during bTB. This could lead to new biomarkers to help genomic selection programs for cattle that are more resistant to bTB as well as new immunostimulation strategies counteracting the type I IFN pathway. This new knowledge will ultimately improve bTB control, a goal which is so greatly needed at the global level (68).

DATA AVAILABILITY STATEMENT

The original contributions presented in the study are included in the article/**Supplementary Material**, further inquiries can be directed to the corresponding author/s.

ETHICS STATEMENT

Ethical review and approval was not required for the animal study because We only used post-mortem sampling at commercial abattoir.

AUTHOR CONTRIBUTIONS

AR designed and did most of the experiments, obtained funding, analyzed the data, prepared all the figures, and wrote the manuscript. FC performed experiments and prepared the inocula for experimental infections under BSL3 conditions. AC cultured AMPs and performed ELISA and q-RT-PCR. ED-D helped in PCLS experiments and revised the figures. MB provided the

Mb3601 strain and revised the manuscript. AA provided the strain Mtb BTB1558. JB improved the RNA extraction protocol. DD and QM performed multiple experiments, and revised the manuscript. FA provided Ab and critically reviewed the imaging data. PG helped with transcriptomic analysis and revised the manuscript. SG obtained funding, designed the experiments, and revised the manuscript. NW obtained funding, supervised all aspects of the work, critically analyzed the data, and wrote the manuscript. All the authors read and approved the manuscript before publication.

FUNDING

This work was supported by the Veterinary Biocontained research facility Network (VETBIONET), the ANR EpiLungCell (grant ANR-17-CE20-0018), and FEDER/Region Centre Val de Loire ANIMALT grant (FEDER convention number EX007516, Region Centre convention number 2019-00134936, research program number AE-2019-1850). Mobilities between France and Ireland were supported by the ONE-TB project (PHC Ulysses, funded by Campus France and the Irish Research Council) and the Fédération de Recherche en Infectiologie du Centre Val de Loire (FéRI).

ACKNOWLEDGMENTS

We thank the staff from the Abattoir du Perche Vendômois for valuable access to and assistance for bovine post-mortem sampling. We thank Dr. Bojan Stokjovic for his assistance for some PCLS experiment. We are very grateful to Gillian P. McHugo for the drawing of the type I interferon pathway with Ingenuity Pathway analysis.

SUPPLEMENTARY MATERIAL

The Supplementary Material for this article can be found online at: <https://www.frontiersin.org/articles/10.3389/fvets.2021.696525/full#supplementary-material>

Supplementary Table 1 | Sequences of primers used in this study. The primers were designed, using Geneious software, in intron-spanning regions when possible. The annealing temperature was set at 60°C. Housekeeping genes used as the reference to calculate Δ CT are indicated in the gray boxes.

Supplementary Figure 1 | Age and geographical origin of the cows used in the study. The Charolaise and Blonde d'Aquitaine cows used were between 3 and 11

years old and came from eight different French departments. Two Blonde d'Aquitaine cows came from the same farm in Indre et Loire, and three Charolaise cows came from the same farm in Sarthe. All the other animals are from distinct farms. The data represent the age of individual animals and the median and interquartile range.

Supplementary Figure 2 | Transcriptomic signature after infection with different doses of mycobacteria. Bovine precision-cut lung slices were obtained as described in **Figure 1** and infected with 10^5 , 5×10^5 , 10^6 , or 5×10^6 colony-forming units. The RNA was extracted 2 days post-infection, and *SDC4*, *CXCL1*, *HIF1*, and *OAS1* gene expressions were assessed with the Fluidigm Biomark. Individual data and the mean and standard deviation in each group are presented ($n = 3$ Charolaise). The dotted line represents the level of expression in the uninfected group.

Supplementary Figure 3 | Cytokines/chemokines in precision-cut lung slice (PCLS) supernatants. The protein levels were measured in PCLS supernatant at 2 days post-infection with Multiplex. Individual data and the median and interquartile range in each group are presented ($n = 6$). * $p < 0.05$ (Wilcoxon nonparametric test).

Supplementary Figure 4 | Structure of the bovine precision-cut lung slices (PCLS) under a light microscope. The PCLS were observed under a light microscope (enlargement $\times 40$ to $\times 200$). The PCLS contain numerous alveoli and between one to three bronchioles, with thick and wavy epithelium that can be easily recognized (black asterisk, two views from the same area under two enlargements). Thin blood vessels (red dotted lines) were localized next to the bronchioles and diffused between the alveoli. No blood cells remained inside the endothelium (the cows were bled out at the abattoir). Alveolar macrophages can be seen inside the alveoli (black arrows).

Supplementary Figure 5 | Localization of Mb3601-GFP in bovine precision-cut lung slices (PCLS). The PCLS were fixed at 2 days post-infection with 10^5 colony-forming units of Mb3601-GFP recombinant strain and labeled with anti-pancytokeratine and anti-MHCII antibodies, which, respectively, revealed anti-pancytokeratine and Alexa 555 conjugated secondary Ab. The PCLS were transferred on cover slides and mounted with Fluoromount-GTM mounting medium containing DAPI. **(A)** The 3D images were analyzed with Leica LAS software. Z-stack imaging was performed at $\times 63$ enlargement with a confocal microscope (10–15 μ m in thickness, step size of 0.5–1 μ m). Dotted white lines are drawn on the alveoli structure. **(B,C)** Crosshead sections illustrating Mb3601 inside **(B)** or near **(C)** an alveolar macrophage. X and Y projections are seen on the bottom and to the right of the picture; the intracellular localization of Mb3601-GFP is indicated by color merging (green + red = yellow). The results from one representative animal are shown (a total of $n = 4$ animals were analyzed).

Supplementary Video 1 | Internalization of Mb3601 in alveolar macrophages after precision-cut lung slice (PCLS) *ex vivo* infection. The PCLS was fixed at 2 dpi with 10^5 colony-forming units of Mb3601-GFP recombinant strain and labeled with anti-pancytokeratine and anti-MHCII antibodies, which, respectively, revealed anti-pancytokeratine and Alexa 555 conjugated secondary Ab. The PCLS was transferred on cover slides and mounted with Fluoromount-GTM mounting medium containing DAPI. Z-stack imaging was performed at $\times 63$ enlargement with a confocal microscope. The 3D images were analyzed with Leica LAS software.

REFERENCES

- Downs SH, Prosser A, Ashton A, Ashfield S, Brunton LA, Brouwer A, et al. Assessing effects from four years of industry-led badger culling in England on the incidence of bovine tuberculosis in cattle, 2013–2017. *Sci Rep.* (2019) 9:14666. doi: 10.1038/s41598-019-49957-6
- Pereira A, Reis A, Ramos B, Cunha M. Animal tuberculosis: Impact of disease heterogeneity in transmission, diagnosis and control. *Transbound Emerg Dis.* (2020) 67:1828–46 doi: 10.1111/tbed.13539
- Hauer A, De Cruz K, Cochard T, Godreuil S, Karoui C, Henault S, et al. Genetic evolution of *Mycobacterium bovis* causing tuberculosis in livestock and wildlife in France since 1978. *PLoS ONE.* (2015) 10:e0117103. doi: 10.1371/journal.pone.0117103
- Reveillaud E, Desvaux S, Boschioli ML, Hars J, Faure E, Fediaevsky A, et al. Infection of wildlife by *Mycobacterium bovis* in France assessment through a national surveillance system, sylvatub. *Front Vet Sci.* (2018) 5:262. doi: 10.3389/fvets.2018.00262
- Harding E. WHO global progress report on tuberculosis elimination. *Lancet Respir Med.* (2020) 8:19. doi: 10.1016/S2213-2600(19)30418-7
- Cole S, Brosch R, Parkhill J, Garnier T, Churcher C, Harris D, et al. Deciphering the biology of *Mycobacterium tuberculosis* from the complete genome sequence. *Nature.* (1998) 393:537–44. doi: 10.1038/31159
- Whelan AO, Coad M, Cockle PJ, Hewinson G, Vordermeier M, Gordon SV. Revisiting host preference in the *Mycobacterium tuberculosis* complex: experimental infection shows *M. tuberculosis* H37Rv to be avirulent in cattle. *PLoS One.* (2010) 5:e8527. doi: 10.1371/journal.pone.0008527

8. Magee DA, Conlon K, Nalpas NC, Browne JA, Pirson C, Healy C, et al. Innate cytokine profiling of bovine alveolar macrophages reveals commonalities and divergence in the response to *Mycobacterium bovis* and *Mycobacterium tuberculosis* infection. *Tuberculosis (Edinb)*. (2014) 94:441–50. doi: 10.1016/j.tube.2014.04.004
9. Ameni G, Vordermeier M, Firdessa R, Aseffa A, Hewinson G, Gordon SV, et al. *Mycobacterium tuberculosis* infection in grazing cattle in central Ethiopia. *Vet J*. (2011) 188:359–61. doi: 10.1016/j.tvjl.2010.05.005
10. J.M. van den Berg, van Koppen E, Ahlin A, Belohradsky BH, Bernatowska E, Corbeel L, et al. Chronic granulomatous disease: the European experience. *PLoS ONE*. (2009) 4:e5234. doi: 10.1371/journal.pone.0005234
11. Garnier T, Eiglmeier K, Camus JC, Medina N, Mansoor H, Pryor M, et al. The complete genome sequence of *Mycobacterium bovis*. *Proc Natl Acad Sci USA*. (2003) 100:7877–82. doi: 10.1073/pnas.1130426100
12. Malone KM, Farrell D, Stuber TP, Schubert OT, Aebersold R, Robbe-Austerman S, et al. Updated Reference Genome Sequence and Annotation of *Mycobacterium bovis* AF2122/97. *Genome Announc*. (2017) 5:e00157–17. doi: 10.1128/genomeA.00157-17
13. Villarreal-Ramos B, Berg S, Whelan A, Holbert S, Carreras F, Salguero FJ, et al. Experimental infection of cattle with *Mycobacterium tuberculosis* isolates shows the attenuation of the human tubercle bacillus for cattle. *Sci Rep*. (2018) 8:894. doi: 10.1038/s41598-017-18575-5
14. Smith N, Berg S, Dale J, Allen A, Rodriguez S, Romero B, et al. European 1: a globally important clonal complex of *Mycobacterium bovis*. *Infect Genet Evol*. (2011) 11:1340–51. doi: 10.1016/j.meegid.2011.04.027
15. Branger M, Loux V, Cochard T, Boschirolu M, Biet F, Michelet L. The complete genome sequence of *Mycobacterium bovis* Mb3601, a SB0120 spoligotype strain representative of a new clonal group. *Infect Genet Evol*. (2020) 82:104309. doi: 10.1016/j.meegid.2020.104309
16. Hauer A, Michelet L, Cochard T, Branger M, Nunez J, Boschirolu ML, et al. Accurate phylogenetic relationships among *Mycobacterium bovis* strains circulating in France based on whole genome sequencing and single nucleotide polymorphism analysis. *Front Microbiol*. (2019) 10:955. doi: 10.3389/fmicb.2019.00955
17. Brosch R, Gordon SV, Garnier T, Eiglmeier K, Frigui W, Valenti P, et al. Genome plasticity of BCG and impact on vaccine efficacy. *Proc Natl Acad Sci USA*. (2007) 104:5596–601. doi: 10.1073/pnas.0700869104
18. Cosma C, Humbert O, Ramakrishnan L. Superinfecting mycobacteria home to established tuberculous granulomas. *Nat Immunol*. (2004) 5:828–35. doi: 10.1038/ni1091
19. Cassidy J. The pathogenesis and pathology of bovine tuberculosis with insights from studies of tuberculosis in humans and laboratory animal models. *Vet Microbiol*. (2006) 112:151–61. doi: 10.1016/j.vetmic.2005.11.031
20. Scordo JM, Knoell DL, Torrelles JB. Alveolar epithelial cells in *Mycobacterium tuberculosis* infection: active players or innocent bystanders? *J Innate Immun*. (2016) 8:3–14. doi: 10.1159/000439275
21. Li Y, Wang Y, Liu X. The role of airway epithelial cells in response to mycobacteria infection. *Clin Dev Immunol*. (2012) 2012:791392. doi: 10.1155/2012/791392
22. Ryndak MB, Laal S. *Mycobacterium tuberculosis* primary infection and dissemination: a critical role for alveolar epithelial cells. *Front Cell Infect Microbiol*. (2019) 9:299. doi: 10.3389/fcimb.2019.00299
23. Thacker VV, Dhar N, Sharma K, Barrile R, Karalis K, McKinney JD. A lung-on-chip model of early *Mycobacterium tuberculosis* infection reveals an essential role for alveolar epithelial cells in controlling bacterial growth. *Elife*. (2020) 9:e59961. doi: 10.7554/eLife.59961
24. Sato K, Tomioka H, Shimizu T, Gonda T, Ota F, Sano C. Type II alveolar cells play roles in macrophage-mediated host innate resistance to pulmonary mycobacterial infections by producing proinflammatory cytokines. *Journal of Infectious Disease*. (2002) 185:1139–47. doi: 10.1086/340040
25. Castillo-Velázquez U, Gomez-Flores R, Tamez-Guerra R, Tamez-Guerra P, Rodríguez-Padilla C. Differential responses of macrophages from bovines naturally resistant or susceptible to *Mycobacterium bovis* after classical and alternative activation. *Vet Immunol Immunopathol*. (2013) 154:8–16. doi: 10.1016/j.vetimm.2013.04.010
26. Queval CJ, Fearnis A, Botella L, Smyth A, Schnettger L, Mitermite M, et al. Macrophage-specific responses to human- and animal-adapted tubercle bacilli reveal pathogen and host factors driving multinucleated cell formation. *PLoS Pathog*. (2021) 17:e1009410. doi: 10.1371/journal.ppat.1009410
27. Goris K, Uhlenbruck S, Schwegmann-Wessels C, Kohl W, Niedorf F, Stern M, et al. Differential sensitivity of differentiated epithelial cells to respiratory viruses reveals different viral strategies of host infection. *J Virol*. (2009) 83:1962–8. doi: 10.1128/JVI.01271-08
28. Marquant Q, Laubret D, Drjac C, Mathieu E, Bouguyon E, Noordine ML, et al. The microbiota plays a critical role in the reactivity of lung immune components to innate ligands. *FASEB J*. (2021) 35:e21348. doi: 10.1096/fj.202002338R
29. Carranza-Rosales P, Carranza-Torres IE, Guzman-Delgado NE, Lozano-Garza G, Villarreal-Trevino L, Molina-Torres C, et al. Modeling tuberculosis pathogenesis through ex vivo lung tissue infection. *Tuberculosis (Edinb)*. (2017) 107:126–132. doi: 10.1016/j.tube.2017.09.002
30. Bryson KJ, Garrido D, Esposito M, McLachlan G, Digard P, Schouler C, et al. Precision cut lung slices: a novel versatile tool to examine host-pathogen interaction in the chicken lung. *Vet Res*. (2020) 51:2. doi: 10.1186/s13567-019-0733-0
31. Thacker T, Palmer M, Waters W. Associations between cytokine gene expression and pathology in *Mycobacterium bovis* infected cattle. *Vet Immunol Immunopathol*. (2007) 119:204–13. doi: 10.1016/j.vetimm.2007.05.009
32. Malone KM, Rue-Albrecht K, Magee DA, Conlon K, Schubert OT, Nalpas NC, et al. Comparative omics analyses differentiate *Mycobacterium tuberculosis* and *Mycobacterium bovis* and reveal distinct macrophage responses to infection with the human and bovine tubercle bacilli. *Microb Genom*. (2018) 4:1. doi: 10.1099/mgen.0.000163
33. Allen AR, Minozzi G, Glass EJ, Skuce RA, McDowell SW, Woolliams JA, et al. Bovine tuberculosis: the genetic basis of host susceptibility. *Proc Biol Sci*. (2010) 277:2737–45. doi: 10.1098/rspb.2010.0830
34. Abadie V, Badell E, Douillard P, Ensergueix D, Leenen PJ, Tanguy M, et al. Neutrophils rapidly migrate via lymphatics after *Mycobacterium bovis* BCG intradermal vaccination and shuttle live bacilli to the draining lymph nodes. *Blood*. (2005) 106:1843–50. doi: 10.1182/blood-2005-03-1281
35. Berry MPR, Graham CM, McNab FW, Xu Z, Bloch SAA, Oni T, et al. An interferon-inducible neutrophil-driven blood transcriptional signature in human tuberculosis. *Nature*. (2010) 466:973–977. doi: 10.1038/nature09247
36. Moreira-Teixeira L, Mayer-Barber K, Sher A, O'Garra A. Type I interferons in tuberculosis: foe and occasionally friend. *J Exp Med*. (2018) 215:1273–1285. doi: 10.1084/jem.20180325
37. Ji DX, Yamashiro LH, Chen KJ, Mukaida N, Kramnik I, Darwin KH, et al. Type I interferon-driven susceptibility to *Mycobacterium tuberculosis* is mediated by IL-1Ra. *Nat Microbiol*. (2019) 4:2128–35. doi: 10.1038/s41564-019-0578-3
38. Menzies F, Neill S. Cattle-to-cattle transmission of bovine tuberculosis. *Vet J*. (2000) 160:92–106. doi: 10.1016/S1090-0233(00)90482-9
39. Neupane A, Willson M, Krzysztof Chojnacki A, F. Patrolling alveolar macrophages conceal bacteria from the immune system to maintain homeostasis. *Cell*. (2020) 183:110–25. doi: 10.1016/j.cell.2020.08.020
40. Queval CJ, Brosch R, Simeone R. The macrophage: a disputed fortress in the battle against *Mycobacterium tuberculosis*. *Front Microbiol*. (2017) 8:2284. doi: 10.3389/fmicb.2017.02284
41. Wedlock D, Kawakami R, Koach J, Buddle B, Collins D. Differences of gene expression in bovine alveolar macrophages infected with virulent and attenuated isogenic strains of *Mycobacterium bovis*. *Int Immunopharmacol*. (2006) 6:957–61. doi: 10.1016/j.intimp.2006.01.003
42. Ferguson J, Schlesinger L. Pulmonary surfactant in innate immunity and the pathogenesis of tuberculosis. *Tuber Lung Dis*. (2000) 80:173–84. doi: 10.1054/tuld.2000.0242
43. Cassidy J, Martineau A. Innate resistance to tuberculosis in man, cattle and laboratory animal models: nipping disease in the bud? *Comp Pathol*. (2014) 151:291–308. doi: 10.1016/j.jcpa.2014.08.001
44. Palmer MV, Wiarda J, Kanipe C, Thacker TC. Early pulmonary lesions in cattle infected via aerosolized *Mycobacterium bovis*. *Vet Pathol*. (2019) 56:544–554. doi: 10.1177/0300985819833454
45. Martineau AR, Newton SM, Wilkinson KA, Kampmann B, Hall BM, Nawroly N, et al. Neutrophil-mediated innate immune resistance to mycobacteria. *J Clin Invest*. (2007) 117:1988–94. doi: 10.1172/JCI31097

46. McCorry T, Whelan A, Welsh M, McNair J, Walton E, Bryson D, et al. Shedding of *Mycobacterium bovis* in the nasal mucus of cattle infected experimentally with tuberculosis by the intranasal and intratracheal routes. *Vet Record*. (2005) 157:613–8. doi: 10.1136/vr.157.20.613
47. Su F, Liu X, Liu G, Yu Y, Wang Y, Jin Y, et al. Establishment and evaluation of a stable cattle type II alveolar epithelial cell line. *PLoS ONE*. (2013) 8:e76036. doi: 10.1371/journal.pone.0076036
48. Lee DE, Stewart GR, Chambers MA. Modelling early events in *Mycobacterium bovis* infection using a co-culture model of the bovine alveolus. *Sci Rep*. (2020) 10:18495. doi: 10.1038/s41598-020-75113-6
49. Ameni G, Aseffa A, Engers H, Young D, Gordon S, Hewinson G, et al. High prevalence and increased severity of pathology of bovine tuberculosis in Holsteins compared to zebu breeds under field cattle husbandry in central Ethiopia. *Clin Vaccine Immunol*. (2007) 14:1356–61. doi: 10.1128/CVI.00205-07
50. Raphaka K, Sanchez-Molano E, Tsairidou S, Anacleto O, Glass EJ, Woolliams JA, et al. Impact of genetic selection for increased cattle resistance to bovine tuberculosis on disease transmission dynamics. *Front Vet Sci*. (2018) 5:237. doi: 10.3389/fvets.2018.00237
51. Banos G, Winters M, Mrode R, Mitchell AP, Bishop SC, Woolliams JA, et al. Genetic evaluation for bovine tuberculosis resistance in dairy cattle. *J Dairy Sci*. (2017) 100:1272–1281. doi: 10.3168/jds.2016-11897
52. Raphaka K, Matika O, Sanchez-Molano E, Mrode R, Coffey MP, Riggio V, et al. Genomic regions underlying susceptibility to bovine tuberculosis in Holstein-Friesian cattle. *BMC Genet*. (2017) 18:27. doi: 10.1186/s12863-017-0493-7
53. Richardson IW, Berry DP, Wiencko HL, Higgins IM, More SJ, McClure J, et al. A genome-wide association study for genetic susceptibility to *Mycobacterium bovis* infection in dairy cattle identifies a susceptibility QTL on chromosome 23. *Genet Sel Evol*. (2016) 48:19. doi: 10.1186/s12711-016-0197-x
54. Ring SC, Purfield DC, Good M, Breslin P, Ryan E, Blom A, et al. Variance components for bovine tuberculosis infection and multi-breed genome-wide association analysis using imputed whole genome sequence data. *PLoS ONE*. (2019) 14:e0212067. doi: 10.1371/journal.pone.0212067
55. Wilkinson S, Bishop SC, Allen AR, McBride SH, Skuce RA, Bermingham M, et al. Fine-mapping host genetic variation underlying outcomes to *Mycobacterium bovis* infection in dairy cows. *BMC Genomics*. (2017) 18:477. doi: 10.1186/s12864-017-3836-x
56. Abel L, Fellay J, Haas DW, Schurr E, Srikrishna G, Urbanowski M, et al. Genetics of human susceptibility to active and latent tuberculosis: present knowledge and future perspectives. *Lancet Infect Dis*. (2018) 18:e64–e75. doi: 10.1016/S1473-3099(17)30623-0
57. Allen A. One bacillus to rule them all?—Investigating broad range host adaptation in *Mycobacterium bovis*. *Infect Genet Evol*. (2017) 53:68–76. doi: 10.1016/j.meegid.2017.04.018
58. J. Sabio Y, García, Bigi MM, Klepp LI, García EA, Blanco FF, Bigi F. Does *Mycobacterium bovis* persist in cattle in a non-replicative latent state as *Mycobacterium tuberculosis* in human beings? *Vet Microbiol*. (2020) 247:108758. doi: 10.1016/j.vetmic.2020.108758
59. Gonzalo-Asensio J, Malaga W, Pawlik A, Astarie-Dequeker C, Passemar C, Moreau F, et al. Evolutionary history of tuberculosis shaped by conserved mutations in the PhoPR virulence regulator. *Proc Natl Acad Sci USA*. (2014) 111:11491–6. doi: 10.1073/pnas.1406693111
60. Huynh K, Joshi S, Brown E. A delicate dance: host response to mycobacteria. *Curr Opin Immunol*. (2011) 23:464–72. doi: 10.1016/j.coi.2011.06.002
61. Russell DG. *Mycobacterium tuberculosis* and the intimate discourse of a chronic infection. *Immunol Rev*. (2011) 240:252–68. doi: 10.1111/j.1600-065X.2010.00984.x
62. Nalpas NC, Magee DA, Conlon KM, Browne JA, Healy C, McLoughlin KE, et al. RNA sequencing provides exquisite insight into the manipulation of the alveolar macrophage by tubercle bacilli. *Sci Rep*. (2015) 5:13629. doi: 10.1038/srep13629
63. Jensen K, Gallagher IJ, Johnston N, Welsh M, Skuce R, Williams JL, et al. Variation in the early host-pathogen interaction of bovine macrophages with divergent *Mycobacterium bovis* strains in the United Kingdom. *Infect Immun*. (2018) 86:e00385-17. doi: 10.1128/IAI.00385-17
64. Palmer M, Thacker T, Rabideau M, Jones G, Kanipe C, Vordermeier H, et al. Biomarkers of cell-mediated immunity to bovine tuberculosis. *Vet Immunol Immunopathol*. (2020) 220:109988. doi: 10.1016/j.vetimm.2019.109988
65. Chunfa L, Xin S, Qiang L, Sreevatsan S, Yang L, Zhao D, et al. The Central Role of IFI204 in IFN-beta Release and Autophagy Activation during *Mycobacterium bovis* Infection. *Front Cell Infect Microbiol*. (2017) 7:169. doi: 10.3389/fcimb.2017.00169
66. Liu C, Yue E, Yang Y, Cui Y, Yang L, Zhao D, et al. AIM2 inhibits autophagy and IFN- β production during *M. bovis* infection. *Oncotarget*. (2016) 7:46972–87. doi: 10.18632/oncotarget.10503
67. Wang J, Hussain T, Zhang K, Liao Y, Yao J, Song Y, et al. Inhibition of type I interferon signaling abrogates early *Mycobacterium bovis* infection. *BMC Infect Dis*. (2019) 19:1031. doi: 10.1186/s12879-019-4654-3
68. Olea-Popelka F, Muwonge A, Perera A, Dean A, Mumford E, Erlacher-Vindel E, et al. Zoonotic tuberculosis in human beings caused by *Mycobacterium bovis*—a call for action. *Lancet Infect Dis*. (2017) 17:e21–e25. doi: 10.1016/S1473-3099(16)30139-6

Conflict of Interest: The authors declare that the research was conducted in the absence of any commercial or financial relationships that could be construed as a potential conflict of interest.

The handling editor declared a past collaboration with one of the authors SG.

Copyright © 2021 Remot, Carreras, Coupé, Doz-Deblauwe, Boschioli, Browne, Marquant, Descamps, Archer, Aseffa, Germon, Gordon and Winter. This is an open-access article distributed under the terms of the Creative Commons Attribution License (CC BY). The use, distribution or reproduction in other forums is permitted, provided the original author(s) and the copyright owner(s) are credited and that the original publication in this journal is cited, in accordance with accepted academic practice. No use, distribution or reproduction is permitted which does not comply with these terms.